Visible light-induced photocatalysis through surface-plasmon excitation of gold on titania surface

Ewa Kowalska,*[a,b,§] Orlando Omar Prieto Mahaney,[a] Ryu Abe[a] and Bunsho Ohtani[a]

Received (in XXX, XXX) Xth XXXXXXXXX 200X, Accepted Xth XXXXXXXXX 200X

First published on the web Xth XXXXXXXXX 200X

DOI: 10.1039/b000000x

Fifteen commercial titania (titanium(IV) oxide; TiO_2) powders were modified with gold by photodeposition to prepare photocatalysts that work under irradiation with light in the visible range (vis). The gold-modified titania (Au/TiO_2) powders were characterized by diffuse reflectance spectroscopy (DRS), field-emission scanning electron microscopy (FE-SEM), scanning transmission microscopy (STEM) and X-ray powder diffraction analysis (XRD). It was shown that all tested powders could absorb visible light with an absorption maximum at localized surface plasmon resonance (LSPR) wavelengths (530-600 nm) and that the size and shape of gold nanoparticles determined absorption ranges. The photocatalytic activity of Au/TiO_2 powders was examined both under ultraviolet and vis irradiation (mainly >450 nm) for acetic acid and 2-propanol photooxidation. It was found that the activity depended strongly on gold and titania properties, such as particle size and shape, surface area and crystalline form. Under vis irradiation, large rutile particles loaded with gold particles of a wide range of sizes showed the highest level of photocatalytic activity, possibly due to greater light absorption ability in a wide wavelength range resulting from transverse and longitudinal LSPR of rod-like gold particles. Action spectrum analyses showed that visible light-induced oxidation of organic compounds by aerated gold-titania suspensions was initiated by excitation of LSPR absorption of gold. Although photocatalytic activity of nanosized gold particles under vis irradiation with a wavelength of ca. 430 nm and catalytic activity of gold-modified titania during dark reaction were also found, it was shown that the activities of

Au/TiO_2 particles originated from activation of LSPR of gold by light of wavelength of 530-650 nm. Participation of molecular oxygen as an electron acceptor and titania as a conductor of electrons was suggested by comparison with results obtained under deaerated conditions and results obtained using a system containing gold-deposited silica instead of gold-titania, respectively. On the basis of these results, the mechanism of visible light-induced oxidation of organic compounds on gold-titania is proposed.

Introduction

Titanium(IV) oxide (TiO_2; titania) is an inexpensive particulate material that is readily available and has substantial photocatalytic activity, stability toward inorganic and organic compounds and non-toxicity.[1] However, one drawback of titania is that it can only be excited by ultraviolet light, i.e., with wavelengths shorter than ca. 400 nm. Therefore, only a very small portion of solar radiation (3-5%) can be utilized to drive chemical reactions.[2] Thus, extension of its absorption wavelength range to the visible region (vis) is an important issue. Another important issue is improvement of quantum efficiency, i.e., an efficiency of utilization of the photoexcited state of photocatalysts, since an electronic excited state of titania is deactivated by recombination of electrons and holes to lower quantum efficiency.[3] Modification of titania with inorganic[4] and organic[5] compounds has often been used to enhance its photocatalytic activity and to extend its absorption wavelength from UV to vis. Surface modifications seem preferable to bulk modifications, such as doping of nitrogen,[4c, 6] sulfur,[7] carbon[6a, 8] or boron,[9] since the doping may produce recombination centers in the crystalline lattice, resulting in a decrease in photocatalytic activity, especially under UV irradiation, though photocatalytic activities under vis irradiation to some extent have been observed. Noble metals and their compounds have been used as surface modifiers, primarily because they possibly inhibit charge recombination by accelerating transfer of photoexcited electrons from titania to substrates, e.g., protons to evolve hydrogen (H_2).[10] In a similar way,[11] platinum nanoparticles loaded on tungsten(VI) oxide also catalyze reduction of molecular oxygen (O_2) into water or hydrogen peroxide through multielectron processes. Another recently

found advantageous function of compounds containing noble metals is their absorption to induce photocatalytic reaction under visible-light irradiation.[12] For example, a platinum complex fixed on titania oxidizes organic compounds through visible light absorption.[12a,b]

Another example of functions of noble metals is photocatalytic reaction driven by possible photoexcitation of surface plasmon (SP) of noble-metal nanoparticles. Gold-modified titania (Au/TiO_2) photocatalysts have exhibited activity under visible-light (> 420 nm) irradiation as reported in several papers.[13] There are two types of SP: localized (localized surface plasmon resonance, LSPR) and propagating (surface plasmon polaration; SPP) ones, depending on the form of noble metal.[14] LSPR occurs in small nanoparticles (10-200 nm), in which light absorption (and amplification of the electric field) has been shown to depend strongly on particle size, shape and local dielectric environment,[15] while SPP is associated with smooth thin films of silver and gold with thicknesses in the range of 10-200 nm. This article focuses on photoactivity under vis irradiation by excitation of the former one.

Noble metal-loaded titania photoreaction systems seem advantageous compared with other photosensitization systems using organic dyes or metal complexes,[16] since noble metal deposits are robust and relatively stable even under photoirradiation in the presence of oxygen. Noble metals can be introduced to surfaces of titania in a reduced metalic state by various methods such as electrolysis,[17] chemical reduction,[18] UV photoreduction,[19] γ-radiation,[20] deposition from colloids or adsorption of metal clusters.[12c, 21] Thus, the combination of titania and noble metal deposits is feasibly achieved.

On the other hand, the mechanism of vis-photoinduced reaction of noble metal-deposited titania has not been fully clarified. As pointed out in a recent review on photocatalysis,[2] the most straightforward and reliable proof that a certain material works as a photocatalyst is resemblance of the action spectrum, wavelength dependence of apparent quantum efficiency, and absorption spectrum. Although it has been reported that an action spectrum for photocurrent, but not reaction products, of Au/TiO_2 electrodes resembles their diffuse reflectance spectrum,[13a] there have been no reports so far, except

for our recent communication,[13d] showing that LSPR excitation actually induced photocatalytic chemical reaction. However, there is still uncertainty in the reaction pathways following the LSPR photoexcitation suggested by action spectrum analysis. The purpose of this study was to elucidate the mechanism of photocatalytic reaction on Au/TiO_2 under vis irradiation by examining action spectra and to determine the properties of photocatalysts required for a high level of activity.

Experimental

Materials

Powdery samples of titania listed in Table 1 with their physical properties were used in this study. Silica (SiO_2, KE-P50, Nippon Shokubai) was also used for a reference. Hydrogen tertrachloroaurate(III) tetrahydrate ($HAuCl_4 \cdot 4H_2O$) (Nacalai Tesque and Wako Pure Chemical Industry) were used as received for metal loadings. Methanol, acetic acid, 2-propanol, acetone, a gold standard solution, L-ascorbic acid and D-ascorbic acid, hydrochloric acid (HCl) and sodium hydroxide (NaOH) (Wako Pure Chemical Industry) were used without further purification.

Generally, 2wt% of gold, which corresponds to 0.81mol% to titania, was photodeposited onto the surfaces of commercial titania powders with different physical properties and crystalline forms (anatase or rutile) by the procedure briefly described below.

Au/TiO_2 powder was prepared simultaneously in eight Pyrex tubes to obtain a sufficient amount of photocatalyst powders. In each tube, 572 mg of titania powder was suspended in 28.6 mL 50vol% aqueous methanol containing $HAuCl_4 \cdot 4H_2O$. The tube was purged of air with argon for at least 15 min and then sealed with a rubber septum. The suspension was photoirradiated with a 400-W high-pressure mercury lamp under magnetic stirring (500 rpm). The temperature of the suspension during photoirradiation was maintained at 298 ± 5 K using a thermostatically controlled water bath. During the irradiation, the amount of generated hydrogen was measured every 15 min by gas

chromatography (Shimadzu GC8A-IT). The thus-obtained Au/TiO_2 photocatalyst was centrifuged, washed at least three times with distilled water, dried overnight at 393 K, and ground in an agate mortar.

Au/TiO_2 particles were also prepared by three variants of the impregnation-reduction method. In the first variant, gold nanoparticles were prepared similarly to the procedure reported by Andreescu *et al.*[22] and were adsorbed on titania and silica powders of similar particle sizes (ca. 0.5 μm). In the second variant, process steps were changed: First, Au(III) cations were adsorbed on the oxides and then chemically reduced. In the third variant, gold nanoparticles were prepared first by chemical reduction, the aggregated larger particles of gold were destabilized during overnight stirring, followed by dissolution with aqua regia. Then Au(III) cations were adsorbed on the oxide surfaces and subjected to consecutive reduction. As a result, 10 modified silica and 8 modified titania powders were obtained. Details of preparation of Au/TiO_2 and Au/SiO_2 powders are shown in ESI.

Characterization of photocatalysts

To characterize the absorption properties of modified photocatalysts, diffuse reflectance (DR) spectra were recorded and data were converted to obtain absorption spectra. DR spectra were taken for both the solid and suspended photocatalysts. The measurements were carried out on a Hamamtsu Photonics C7473-6 photonic multichannel analyzer (barium sulfate and bare titania powders used as references) and on a Jasco V-670 spectrophotometer equipped with a PIN-757 integrating sphere with baseline recorded using a poly(tetrafluoroethylene) reference and bare titania powders.

The morphology of gold photodeposited onto titania was observed by field emission scanning electron microscopy (FE-SEM, JEOL JSM-7400F) and scanning transmission electron microscopy (STEM, Hitachi HD2000 ultrathin film evaluation system). Au/TiO_2 powders were dispersed in, respectively, water and ethanol in an ultrasound bath for a few minutes for SEM and STEM observations, and some drops of suspension were deposited on a piece of copper tape and an amorphous carbon-covered reinforced copper grid (Onken, types A and B), respectively. Some powder samples were

also attached to conductive carbon paint on substrates for SEM observations. The samples prepared by both methods were dried under vacuum overnight. For SEM analyses, images were acquired at a wide range of magnification (30000-600000) in a secondary electron imaging mode (SEI) or a lower electron imaging mode (LEI) witn 3-mm and 6-mm working distances, respectively, 4–5-kV accelerating voltage and 10 μA emission current. For STEM, images were acquired at a wide range of magnification (70000-1800000) in normal, high resolution and ultra high resolution modes with 3- and 2-mm working distances, 200 kV accelerating voltage and 30 μA emission current. Secondary electron (SE), Z-contrast (ZC) and bright-field (BF) images were recorded.

X-ray diffraction (XRD) patterns were recorded on a diffractometer (Rigaku, RINT Ultima+) equipped with a graphite monochromator using copper K_α radiation (40-kV tube voltage and 20-mA tube current). Measurements were carried out with two scan speeds (2 and 0.2° min^{-1}) and three scan ranges (10-90°, 35-40° and 42-47°), the slower one for narrower ranges being used for particle size determination. To determine primary particle sizes of titania (PC101A) and gold deposits, XRD data were calculated using Scherrer's equation with appropriate corrections.[23] The sizes of all titania particles (except PC101A, which was determined in this study) and surface areas (using BET Brunauer, Emmett and Teller (BET) method) were determined by our group previously.[23]

The amount of deposited gold was determined by flame atomic absorption spectroscopy (FAAS, Shimadzu AA-6200). The deposited gold (25 mg as Au/TiO_2) was dissolved by aqua regia (2 mL) under magnetic stirring (250 rpm) for > 1 h, decanted after centrigugation, and poured into a 50-mL volumetric flask. The remaining white titania was rinsed twice with 1 mol L^{-1} HCl (5 mL) under magnetic stirring (10 min, 250 rpm) and centrifuged. The resultant supernatant was added to the aqua regia solution of gold followed by the addition of 1-mol L^{-1} HCl. Gold calibration solutions were prepared from a gold standard solution by dilluting with 1-mol L^{-1} HCl.

Photocatalytic activity tests with polychromatic irradiation

Irradiation with UV and/or vis using a mercury lamp

A metal-loaded photocatalyst (50 mg) was suspended in aqueous solutions of acetic acid and 2-propanol (5vol%, 5 mL) and photoirradiated under magnetic stirring (1000 rpm) in the same set-up as that for used the gold photodeposition with the exception of the test-tube holder, which was changed to enable irradiation of 12 thinner tubes at the same time. For the test of visible light-induced activity, the test-tube holder was changed to four test-tube holders (each holder containing two sample tubes) with cut-off filters (Y48, Asahi Techno Glass) mounted in the irradiation window so that light of wavelengths > 450 nm reached the suspensions. During the irradiation of acetic acid solutions, a portion (0.2 mL) of the gas phase of the reaction mixture was withdrawn with a syringe and subjected to gas chromatographic analysis of carbon dioxide (CO_2) (Shimadzu GC-14B equipped with a flame ionization detector and a methanizer (Shimadzu MTN-1)). Due to the relatively small yield of CO_2 under vis irradiation, enhancement of FID sensitivity by converting CO_2 into methane in the methanizer was required. For the irradiated samples with 2-propanol solutions, the generated acetone was analyzed using a Shimadzu GC-14B gas chromatograph equipped with a flame ionization detector. Before injection of a portion of liquid phase to GC, the photocatalyst powder was separated from the suspension using a filter (Whatman Mini-UniPrep, PVDF).

Vis irradiation using a xenon lamp

The activity of samples under vis irradiation was also examined using a xenon lamp in two kinds of set-up. In the first one, a sample holder, the same as that used in a mercury lamp set-up, with two tubes was kept in a water bath thermostated at 298 ± 5 K. The contents were magnetically stirred and irradiated by a xenon lamp installed outside the water bath. Due to the tightness of the sample-holder housing to prevent UV-light leakage, the temperature of the cooling water inside the holders increased by at most 18 K during 7-h irradiation. Another set-up (Fig. 1) was also used. The set-up consisted of two parts. In the first part (A), light from a xenon lamp (1) passed through a water bath (8) and then through a UV cut-off filter (3) to eliminate IR and UV radiation, respectively. To achieve water circulation through the two parts and to prevent leakage of UV light to part B, a separating wall (5) was mounted in part A to make the circulating water flow over it and

then through a hole (9) in the partition wall between the two parts. In part (B), two test-tubes (12) were mounted behind the filter at the same distance from the light source. Their contents were stirred (13) and cooled by the circulating water.

Monochromatic irradiation — action spectrum analysis

For action spectra analyses, a 20-mg portion of photocatalyst was suspended in 2 mL of aqueous acetic acid or 2-propanol (5vol%) and irradiated for 1-5 h using a diffraction grating type illuminator (Jasco CRM-FD) equipped with a 300-W xenon lamp (Hamamatsu Photonics C2578-02). The intensity of irradiation, measured by a Molectron PM5200 laser power meter or a Hioki 3664 optical power meter, was in the range of 1.24–3.9×10^{-8} einstein s^{-1}. Since the rate of photocatalytic reactions, especially those including molecular oxygen, depend on the intensity and on the wavelength,[24] the light flux should be adjusted to be the same, independent of the wavelength. However, in these experiments, the light intensities at terminal wavelengths (> 700 nm, not crucial for our analysis) were very low (almost 3 times lower than at 460-600 nm) and adjustment of light intensities to this level was connected with reaction rate decreased and thus with experimental error increased. In this regard, no irradiation intensity adjustment was performed. Full-width at half-maximum (FWHM) of the monochromatic light was ca. 15 nm irrespective of the wavelength. During experiments, reaction mixtures were continuously stirred. The stoichiometries of acetic acid and 2-propanol oxidations are assumed to be follows.

$$CH_3COOH + 2O_2 \rightarrow 2CO_2 + 2H_2O$$

$$2(CH_3)_2CHOH + O_2 \rightarrow 2(CH_3)_2CO + 2H_2O$$

Apparent quantum yield was calculated as the ratio of the rate of electron consumption from the rate of acetone or CO_2 generation to the flux of incident photons, assuming that 4 and 2 photons, respectively, are required. Dark reactions in a cuvette thoroughly covered with aluminum foil were also carried out, and the thus-obtained rates of dark reactions

were substracted from the rates observed under photoirradiation.

Results and discussion

Gold photodeposition

During the photodeposition process using methanol as a sacrificial hole scavenger under UV photoirradiation, monotonous liberation of hydrogen was observed after an appreciable induction period (generally < 15 min) for all of the samples (as shown in the inset of Fig. 2), suggesting that gold was reduced to its metallic state to catalyze H_2 evolution. This also means, from our experience of photodeposition of metal particles on titania, that all precursor gold ions had been reduced to metallic gold. Thorough deposition of gold was confirmed by FAAS analyses with the determined amount of gold ranging from 1.95 to 2.1wt% when the source corresponding to 2wt% was used for deposition. It was also observed that, regardless of the amount of gold used for deposition, all gold in the range of 0.05 to 10wt% was attached to the titania surface. The rate of H_2 evolution as a function of particle size of titania is shown in Fig. 2. The highest reaction rate was achieved for the smallest anatase particles of relatively larger surface area, such as TIO10, ST01, PC101 and PC101A. On the other hand, among rutile titanias, the opposite tendency was noticed, though the difference in activity was small compared to that for anatase-rich titania. The fastest methanol dehydrogenation was observed for large rutile-rich photocatalysts, such as TIO5 and Aldrich_r. It seems that surface area of rutile is not crucial and does not control the reaction rate. In our recent study,[23] it was found from photocatalytic titania activity tests with 35 commecial powders that for photocatalytic dehydrogenation of methanol by platinum-loaded titania, anatase is preferabe and both high crystallinity (i.e., smaller density of latice defects) and larger specific surface area are required for higher level of photocatalytic activity. A possible reason for the better activity of anatase is a slightly more cathodic (negative) position of its conduction-band (CB) bottom compared with that of rutile. Assuming similar dependence of activity of gold/titania particles on their physical properties, specific

surface area and crystallinity seem to predominate for anatase-rich and rutile-rich titanias, respectively.

Characterization of Au/TiO_2

Au/TiO_2 showed different colors, violet, pink and grey, and different color brightnesses, as can be seen in Table 1. Thus, all modified powders gave an LSPR absorption band in vis. Representative spectra and values of peak wavelength of LSPR are shown in Fig. 3 and Table 1, respectively. It has been reported that LSPR absorption appears in near-UV, vis, and near- or mid-infrared (IR) regions depending on the size and shape of gold nanoparticles.[14,15, 25] Therefore, the broad absorption band in the wavelength range around 400-700 nm with a peak positioned in the range of 530-610 nm, corresponding to the observed color of powders, is attributable to LSPR of gold on titania. It was thought that gold particles of smaller sizes were generated on fine titania particles, as the LSPR peaks were observed at shorter wavelengths (530-560 nm). On the other hand, the grey color of large rutile particles, e.g., Aldrich_r and TIO5, absorbing longer wavelength (> 590 nm) light indicates the presence of relatively large gold nanoparticles. For these powders, two main peaks in their absorption spectra are attributed to gold particles with a relatively large size distribution and/or rod-like shapes exhibiting transverse and longitudinal plasmons at 520-530 and 600 nm as has already been reported.[25c,e]

It should be noted that when DR spectra were taken for bare titania as a reference material, small absorption peaks at ca. 320 and 430 nm were detected, suggesting the presence of gold particles of < 2 nm in size;[26] Esumi had observed a broad absorption band with two shoulders at about 310 and 420 nm for gold nanoparticles. Absorption at 300, 400 and 650 nm was also observed by Sharma;[27] absorption at 400 and 650 nm by triangular gold nanoparticles and absorption at 300 nm by a fraction of reducing molecules as a surface passivating agent were suggested.

It is known that LSPR peak position depends also on the solvent.[28] However, DR spectra of Au/TiO_2 suspension in aqueous acetic acid solution (5vol%) and in water showed no significant differences to that of solid samples.

A large size distribution of gold nanoparticles (5-150 nm) on large titania particles was observed in SEM images, as shown in Figs. 4a and b. The size and shape of gold nanoparticles might depend on properties of titania, such as particle sizes, surface defects and uniformity. Unlike large rutile particles, anatase particles of smaller size and with higher density of defects seemed to bear smaller gold particles. Typical gold size distributions on Au/TiO_2 (Aldrich_r and ST01) determined by measuring 115 and 119 particles in SEM and STEM images, respectively, are shown in Fig. 5.

Gold particle size estimated from corrected FWHM of the most intense XRD peaks with Scherrer's equation increased linearly with increase in titania particle size estimated in a similar way as shown in Table 1. We previously reported the linear dependence of size of gold particles as well as that of peak wavelength of LSPR on the size of titania particles.[13d] It is clear that the larger the size of titania particles is, the larger is the size of gold particles and hence the longer is the peak wavelength of LSPR absorption.[29] This is consistent with the suggestion that defective sites on titania act as nucleation centers of gold,[30] considering that the observed relatively higher density of defects of fine titania particles[23] may produce a larger number of gold nuclei. Deviation from the linear relations between LSPR peak position and titania particle size was seen for TIO5, which gave two peaks in its absorption spectra, indicating the presence of rod-like gold particles exhibiting transverse and longitudinal plasmons at 520-530 and 600 nm.

Photocatalytic activity under UV irradiation

Figure 6 shows photocatalytic activities for acetic acid photodecomposition under UV irradiation. In general, anatase photocatalysts showed higher levels of photocatalytic activity than those of rutile ones, as has frequently been observed,[31] mainly due to a slightly more negative conduction-band bottom of anatase.[23] Such photocatalytic reactions involve reduction of oxygen (O_2) by photoexcited electrons, and its redox potential is close to the conduction-band bottom of titania. The above-mentioned interpretation is supported by the fact that enhancement ratios, i.e., ratios of activities of gold-loaded titania to bare titania, for rutile-rich titanias were generally larger than those

for anatase-rich ones. It is plausible that gold acts as a co-catalyst for reduction of O_2 by photoexcited electrons, as does platinum,[11] though anatase has almost sufficient ability even in the absence of metal loadings.

Photocatalytic activity under vis irradiation

At first, 12 photocatalysts (10 anatase-rich and 2 rutile-rich samples) were prepared and tested. Different from the results under UV irradiation, the highest level of activity under irradiation at wavelengths > 450 nm (Y48 filter) was obtained with large titania particles with small specific surface area. Negligible activity was observed for fine, dark, intensively colored anatase samples with large surface areas, such as ST01, P25 and PC101. To determinate whether polymorphic form or particle size determines activity under vis irradiation, 4 new rutile-rich photocatalysts with different surface properties were modified with gold and examined. The results are summarized in Fig. 7 and ESI, Fig. S6. It was found that particle size of titania/gold is the key factor for high level of activity, and a good correlation between particle size and activity has been found.[13d] A possible reason for the higher level of activity of samples with larger gold particle size is their absorption in a wider wavelength range, leading to a larger number of absorbed photons. Similarly, negligible visible light-induced activity of a gold-modified fine particulate titania sample was observed by Awate *et al.*[32] The opposite dependence, increase in degradation efficiency under vis irradiation with decrease in gold particle size, has also been reported,[33] though gold was deposited only on three kinds of titania particles (P25, synthesized titania, and titania-alumina) of smaller particle size in that study.

To determine whether Au/TiO_2(ST01) exhibits a higher level of activity at shorter wavelengths, at which nanosized particles (< 2 nm) of gold can absorb light (410 nm),[26] experiments were repeated for a wider wavelength range using another cut-off filter, L42 (> 390 nm, ESI, Fig. S5). However, the obtained acetone-generation rate (0.13 μmol h^{-1}) was only slightly higher than that for longer wavelengths (Y48) and much lower than rates obtained for the best rutile powders.

Thus, an excess amount of deposited gold on these fine photocatalysts, resulting in

very dark color, was considered to be a possible cause of their low level of activity. In fact, a decrease in the amount of deposited gold to 0.05 or 0.1wt% resulted in brightly colored powders of slightly higher level of activity. However, the distribution of gold particle sizes for 0.05wt% gold was similar to that of gold deposited in larger amount, and the obtained acetone-generation rate was only a little higher than that for 2wt% (at 0.1wt% loading, rates of 0.076 and 0.090 μmol h^{-1} for ST01 and TIO10, respectively).

It is also thought that unevenness of emission spectra of a mercury lamp, which emits three main intense lines in vis at 436, 547 and 579 nm (ESI, Fig. S5), and thus large differences in irradiation intensities (e.g., 3 and 249 μW cm^2 at 530 and 550 nm, respectively), and resulting mismatching with gold absorption is also considered to be a reason for the lower level of activity of fine anatase powders. In this regard, control experiments with a xenon lamp for five Au/TiO_2 photocatalysts, ST01, TIO10, Aldrich_a, STG1 and Aldrich_r, were carried out. Irradiation of more intense light of power almost constant at whole range of irradiation (250-320 μW cm^2) may lead to a marked increase in the reaction rate for all tested powders. However, the fastest 2-propanol-oxidation rate was still obtained for large rutile powders, e.g., 2.77 μmol h^{-1} by Au/Aldrich_r. The activity levels of fine anatase powders were still very low and reached only 0.36 and 0.42 μmol h^{-1} for ST01 and TIO10, respectively. The largest enhancement of activity by changing the light source from a mercury lamp to a xenon lamp was observed for Aldrich_r (6.4 times), and the ratios for fine anatase powders, ST01 and TIO10, were 5.2 and 5.3 times, respectively. On the other hand, the enhancement ratio of STG1 and Aldrich_a, for which LSPR occurs at almost the same wavelength as that of main mercury lamp emission, was only 3 times. Therefore, to obtain actual data of activity for gold-modified samples of LSPR absorption at different wavelength, the use of an irradiation source with almost constant power in the whole irradiation range, e.g., xenon lamps, is recommended.

The higher level of photocatalytic activity of gold-modified large rutile particles than that of anatase ones might be caused by the properties of gold and/or titania particles, e.g., higher level of activity of larger gold nanoparticles can result from their higher Fermi

energy as has been reported for gold nanoparticles in the range of 3 to 13 nm deposited on titania, for which Fermi energy and photoactivity under UV irradiation increased with increase in particle size.[34] Titania particles can influence the reaction rate directly and indirectly. The direct effect is due to titania properties, such as size, shape, aggregation, surface defects and CB position, while the indirect effect is due to titania-gold interaction, such as complex energetic properties (electron mobility), titania impact on the properties of generated gold, such as size, shape, stablity and (in-)activation, e.g., better visible light-induced activity of gold-modified rutile samples can be caused by their lower (0.2 eV)[35] level of CB than that of anatase ones and thus higher possibility of electron transfer from gold to titania. Although this reduces the probability of electron transfer from titania to moleclar oxygen (O_2) to give superoxide ($O_2^{\cdot -}$).[36] However, a reduced charge state of oxygen close to O_2^{2-} adsorbed on titania (110) after titania modification with gold has been reported.[36] The possibility of direct electron transfer from gold to oxygen should also be considered, and the necessity of semiconductor presence in the system must be confirmed (and is reported in the next paragraph). The observed higher level of activity of titania with larger gold nanoparticles could also be caused by easier electron transfer between gold and titania particles, as a larger shift of O 2p nonbonding peak towards the Fermi level for larger gold particles has been observed.[37] The back electron transfer from titania to gold resulting in a decrease in reaction rate should also be considered. Recently, it has been reported that for titania particles of different sizes (9, 20, 30 and 50 nm) modified with gold nanoparticles of the same size (10 nm), the best activity under vis irradiation was achieved for larger titania particles for which longer charge recombination time was observed, due to longer diffussion length of electrons in those titania particles.[38]

Mechanistic studies

The mechanism of decomposition of colorless organic compounds (OCs; 2-propanol and acetic acid) under vis irradiation over Au/TiO_2 similar to the activation of sensitizers, such as metal complexes or dyes,[8c,12] is proposed. First, incident photons can be absorbed by gold particles through their LSPR excitation. Then an electron is injected from the gold particles

into the CB of titania and reduces molecular oxygen adsorbed on the surface of titania, and the resultant electron-deficient gold could oxidize organic compounds to be recovered to the original metallic state.

(1) Step one — Absorption (Action spectrum analyses)

In order to clarify the initial step of photoinduced reaction, i.e., what absorbs light to initiate the reaction, action spectrum (AS) analyses were performed.

Representative action spectra for Au/TiO_2(Aldrich_r)[13d] and Au/TiO_2(Au/ST41) are shown in Figs. 8 and 9, respectively. All of the tested Au/TiO_2 samples gave action spectra that resembled respective absorption spectra measured in a diffuse reflection mode; the action and absorption spectra of each sample coincided in their peak positions, ca. 570-600 nm. For clarity, the absorption spectra were shifted along the vertical axis as has been employed for similar spectral comparison in Au/TiO_2 electrode systems.[13a] It is reasonable to conclude that the photoinduced oxidation of 2-propanol into acetone is driven by LSPR of gold and the broad LSPR peak in each absorption spectrum is superimposed on light-scattering inducing no photochemical reactions.

The fine structure of action spectra for which the broad peaks are composed of a few narrow peaks with widths of ca. 30-50 nm is attributable to activities of gold particles of characteristic size and/or shape, depending strongly on absorption intensity at each wavelength, as full width at half maximum (FWHM) of monochromatic light used for the action spectrum analyses was ca. 15 nm, which was sufficiently large to obtain a smooth spectrum, compared with FWHM of the absorption measurement. This behavior indicates that the reaction order of 2-propanol oxidation can be higher than 1 and might be proved by detailed examination of the reaction rate in the function of incident light intensity. However, the activity level under vis irradiation was too low to measure correctly at the lower intensity. Thus, 2-propanol decomposition as a function of intensity of incident light is now being studied in a different set-up with much higher light intensity and will soon be reported.

For Au/Aldrich_r, the action spectrum seems to reflect two main absorption maxima of small (ca. 10-25 nm) and larger (ca. 30-60 nm) gold nanoparticles at 530 and

560-610 nm, respectively. Transverse LSPR of rod-like gold nanoparticles is also responsible for the peak at shorter wavelengths. Assuming that the rate of photoreaction depends strongly on the intensity, observation of such fine structures in action spectra is reasonable. The observable activity for longer and shorter wavelengths than LSPR could be caused by the presence of larger and smaller gold nanoparticles, respectively. Thus nanosized gold particles (< 2 nm) could be responsible for the activity at 460 nm. However, it is impossible to analyze this activity because bare titania for this wavelength also exhibited some activity (also confirmed under polychromatic irradiations with xenon and mercury lamps and cut-off filters, data not reported here). While the activity at wavelength above 605 nm might be caused by the presence of very long gold particles (>150 nm). Wang *et al.* observed longitudal plasmon resonance around 1200 nm for nanorice particles of 340 nm in longitudal diameter.[39]

In the case of modified anatase (Au/ST41), the peak of action spectra of 2-propanol oxidation (also confirmed for acetic acid oxidation) was slightly sharper than that of Au/Aldrich_r. This was caused by generation of gold particles of sizes in a narrower range on a more uniform titania surface, resulting in a narrower LSPR peak, though clear peak maxima at 530-545, 575 and 620 nm probably corresponding to gold particles of 15-25, 31-50 and 61-80 nm, respectively, were observed.

In addition to the photoactivity of titania modified with gold nanoparticles, we were also interested in the possibility of photoinduecd reaction on titania with nanosized (1-2 nm) gold deposits. Although catalytic reactions on nanosized gold have been well known,[40] there is no report on its photocatalytic activity. To determine whether nanosized gold can also exhibit photocatalytic activity under vis irradiation, action spectrum analysis for Au/Aldrich_a, for which a bare photocatalyst showed inactivity at wavelengths longer than 420 nm, was carried out. The quantum yields of 2-propanol oxidation on titania with nanosized gold and gold nanoparticles at 450 and 570 nm, respectively, are shown in Fig. 10. Although the possible advantages of usage of nanosized gold caused by: decreased the energetic difference between the d-band threshold and the Fermi edge;[41] higher shift in the apparent Fermi level of the TiO_2-Au composites to more negative potential [42]

occurence of a metal-to-nonmetal transition[40b] thus gold particles are expected to be semiconducting rather than metallic and a mechanism, based on semiconductor-semiconductor contact (in which photoexcited electrons are injected from gold into the titania CB creating separated electrons and holes which then undergo charge transfer reactions with adsorbates) can be considered;[43] Schottky junction formation (leading to Au-to-TiO_2 electron transfer)[43,44] are well known, our results show that titania modified with gold nanoparticles resulted in much higher Φ_{app} than did titania modified with nanosized gold. It should be noted that Φ_{app} is composed of two self-contained parts, i.e., efficiency of absorption and efficiency of electron-hole utilization.[45] Therefore, even if the efficiency of absorption is constant, i.e., in the case of application of the same photocatalyst, different action spectra can be obtained due to different yields of charge carriers utilization. Thus, higher Φ_{app} of titania with gold nanoparticles can be caused either by better efficiency of photon absorption or by faster electron transfer and its utilization on larger gold deposits. It has been shown that extinction at short wavelengths is due mainly to absorption, not scattering,[46] and thus high efficiency of absorption for nanosized gold is expected. Therefore, the much lower Φ_{app} is attributted to poorer electron utilization depending also on nanoparticle size.[48]

Another feature of the action spectra of Au/TiO_2 photocatalysts is the lowest Φ_{app} at wavelengths of about 485-490 nm (between the activity of nanosized gold and LSPR), which originates from the "spillout" effect that occurs for small cluster sizes (< 5 nm), for which average electron density is reduced with decreasing cluster size.[25d] In this regard, it can be concluded that for photoinduced oxidation of OCs on titania modified with gold of size larger than 5 nm should be used.

(2) Step two — electron in conduction band of titania

After absorption of incident photons by gold particles through their LSPR excitation, as was proved by action spectrum analyses, there are two possible ways for an electron to be in CB of titania.

(a) An electron may be injected from gold particles into the CB of titania and then reduce molecular oxygen adsorbed on the surface of titania, while electron-deficient metal can

oxidize OCs to be recovered to its metallic state.[13d] A similar route was also proposed for an organic solar cell system composed of ZnPc/Ag/ITO, in which it was assumed that "free" electron gas transfers energy to one electron, which in its exited state can fill the empty state of ITO (in our case CB of titania), if it has momentum perpendicular to the contact area, and at the same positive charge, the empty state left in the metal particle has to be filled again with an electron from ZnPc (in our case from OCs);[47] Furube *et al.* reported direct observation of electron transfer from gold nanodots to titania particles using femtosecond transient absorption spectroscopy with an IR probe.[48] However, estimated reaction time (240 fs) seemed to be much longer than the lifetime of the gold LSPR excitation state, presumably caused by limited time resolution of their instrumental setups. Using a setup with time resolution < 50 fs, direct electron transfer from gold to titania was suggested.[39] Very recently, Sakai *et al.* also reported generation of a cathodic photocurrent on an ITO/Au/TiO_2 electrode, supporting the occurrence of electron transfer from plasmon-excited gold nanoparticles to titania.[49]

(b) Excitation of titania by electric near-field of LSPR resulting in electron-hole generation.[50]

To check which hypothesis is correct, we examined indirect modification of titania with gold through connection with thiol groups, as we previously used for heterodimeric particle assemblies of a silica-gold-silica structure.[51] If hypothesis (b) is correct, direct deposition of gold on the titania surface (electronic contact) would not be necessary, as LSPR is observed up to tens of nanometers from the gold nanoparticle.[41] However, preliminary results suggest that direct electron transfer from gold to titania as the reaction rate was dramatically decreased by deposition of gold on the modified titania surface. The details will be published in a forthcoming paper.

There is also the possibility that the mechanism of electron transition depends on the surface properties of particles, as was reported for silver films with different roughnesses; on films with a rough surface, a 2-photon process is mediated by excitation of LSPR and it involves indirect, momentum non-conserving transition, while on smooth films, photoemission is induced by 1-photon and 2-photon processes.[52]

(3) Step three — oxygen reduction

After electron injection from gold particles into the CB of titania, it is thought that an electron can reduce molecular oxygen adsorbed on the surface of titania. Therefore, the necessity of the semiconducting material (titania) and oxygen in photocatalytic decomposition of OCs on gold-modified supports was examined in control experiments with gold deposited on an insulator (silica) and in deaerated conditions, respectively.

For comparison, silica and titania of similar primary particle sizes (ca. 500 nm) were selected and gold was deposited on them by the impregnation-reduction method from an aqueous solution of $HAuCl_4 \cdot 4H_2O$ using ascorbic acid as a reducing agent for generation of gold nanoparticles with well-defined sizes (see ESI, Figs. S1 and S2). For all eighteen tested powders, with different colors and color intensities, Au/SiO_2 showed much lower levels of activity (usually inactive) than those of Au/TiO_2 prepared in the same way. The acetone-generation rate for the most active Au/SiO_2 reached 0.021 μmol h^{-1} (xenon lamp, > 435 nm, Y44 filter) and was twelve-times lower than that for corresponding Au/TiO_2. The same tendency was noticed during acetic acid decomposition and reaction rates reached 0.77 and 0.13 μmol h^{-1} for respective titania and silica powders (see ESI, Fig. S4). After consideration of contribution of dark decomposition of acetic acid in the absence of photocatalyst (0.08 μmol h^{-1}) the activity of the best Au/SiO_2 was thirteen-times lower (almost the same as in the case of 2-propanol oxidation) than activity of corresponding Au/TiO_2.

It should be noted that during 2-propanol oxidation the highest level of activity (0.25 μmol h^{-1}) of Au/Aldrich_r prepared by this method was slightly lower than that prepared by photodeposition (0.32 μmol h^{-1}), suggesting better electronic contact between gold and titania in the photodeposition method. Since the gold particles deposited by photocatalytic reaction of titania, i.e., reduction of gold(III) ions with photoexcited electrons and subsequent reduction of another Au^{3+} occurred on the gold surface, electronic contact between gold and titania might have been established. Better uniformity in gold size/shape distribution by the impregnation-reduction method and thus narrower LSPR (ESI, Fig. S3) might also be the reason for their lower level of activity.

The possibility of direct photooxidation of OCs on plasmonically activated gold

should also be considered. Recently, Chen *et al.* have reported that gold deposited on oxide supports (SiO_2, CeO_2, Fe_2O_3, ZrO_2) can oxidize OCs under vis irradiation as a result of thermal reaction caused by LSPR.[53] However, on the basis of the results showing much slower reaction on silica than on titania with gold nanoparticles having similar size distributions, it can be concluded that the mechanism invloving electron transfer through the CB of the semiconductor is predominant for efficient decomposition of OCs.

When experiments for Au/Aldrich_r were conducted in deaerated conditions, the reaction proceeded negligibly (less than one tenth) compared with that under aerated conditions. Thus, participation of oxygen as an elecron acceptor was also confirmed.

On the basis of results presented here, the following mechanism of photoinduced oxidation of 2-propanol over Au/TiO_2 is proposed as schematically shown in Fig. 11. First, incident photons are absorbed by gold particles through their LSPR excitation, as was proved by action spectrum analyses. A possible reason for the higher level of activity of samples with larger gold particle size is their absorption in a wider wavelength range, leading to a larger number of absorbed photons. We propose that electrons may be injected from Au particles into the CB of titania and then reduce molecular oxygen adsorbed on the surface of titania. The resultant electron-deficient gold can oxidize organic compounds, such as 2-propanol and acetic acid, to be recovered to its original metallic state. It has been proved that molar amount of the product acetone, ca. 5 μmol, was ca. 40-times larger than that of gold when 0.05wt% Au-loaded titania was used. Thus, photocatalytic action of gold particles was confirmed, for the first time to our knowledge, by the observation of resemblance of action and absorption spectra and turnover number exceeding unity.

Conclusions

The results and discussion presented in this paper led to the following conclusion:

An efficient photocatalyst that is active under both UV and vis irradiation can be obtained by modification of titania with gold nanoparticles. Enhanced activity under UV irradiation indicates the inhibition of charge recombination and thus smooth electron transfer

between titania and gold. Under vis irradiation, LSPR of gold is responsible for the activity of Au/TiO_2 photocatalysts and the presence of a semiconducting material, such as titania, for electron transfer and oxygen as an electron acceptor in the reaction system is necessary. Action spectrum analyses have proved to be a useful tool for elucidation of the mechanism (initial step) of OC oxidation under vis irradiation. Since the electron transfer from gold to titania has not been proved in this study, further experiments to show the necessity of direct contact between gold and titania for efficient reaction and thus existence of direct electron transfer from gold to titania are now in progress. To prove electron transfer from gold to titania, experiments using double-beam photoacoustic spectroscopy[54] with excitation of LSPR and detection of accumulated electrons will also be carried out.

Photocatalytic reaction rate depends strongly on the properties of titania, such as particle size, surface area and crystalline form (anatase or rutile) and on the properties of gold deposits, such as size and shape, which are strictly dependent on titania particle properties, and thus fine gold nanoparticles are generated on fine titania with a large amount of surface defects, while larger gold nanoparticles, due to gold coalescence, are mainly formed on large titania particles. To specify how sizes of gold and titania influence activity, gold nanoparticles with uniform sizes should be deposited on different titanias. In this regard, Au/TiO_2 photocatalysts with controlled size distribution are presently being prepared by the microemulsion method.

Nanosized gold, catalytic activity of which is well known, also shows photocatalytic activity for OCs oxidation when deposited on semiconducting materials. Titania particles modified with gold by photodeposition are also catalytically active during dark reaction, though levels of catalytic activity are much lower than photocatalytic ones during irradiation.

Modification of titania by photodeposition seems to be beneficial in comparison with the impregnation-reduction method, due to possible better electronic contact between gold and titania and due to generation of a wide variety of gold nanoparticles with different sizes and shapes enabling the absorption of visible light in a wider range of wavelengths and thus with higher level of activity.

For comparison of the photocatalytic activities of different Au/TiO_2 powders under vis irradiation, an irradiation source with stable light intensities over the whole irradiation range, such as a xenon lamp, should be used.

Acknowledgements

This research was financially supported by the Japan Society for the Promotion of Science under the FY2005 JSPS Postdoctoral Fellowship for Foreign Researchers, KAKENHI (Grant-in-Aid for Scientific Research) on Priority Area "Strong Photon-Molecule Coupling Fields" (No. 470) and the Global Center of Excellence (GCOE) Program “Catalysis as the Basis for Innovation in Material Science” from the Ministry of Education, Culture, Sports, Science and Technology (MEXT) of Japan, and the Polish Ministry of Science and Higher Education (grant No. N N523 487634). The technical assistance of Dr. F. Amano in preparation of set-up for irradiation and explanation of apparatus functioning is highly acknowledged.

Table 1 Physicochemical properties of Au/TiO_2 photocatalysts

Name[a]	Supplier[b]	Crystalline form[c]	Color[d]	LSPR /nm	Particle size/nm	
					titania	gold
ST01	Ishihara	A	d. pink	538	8[e]	9
TIO10	CSJ	A	violet	558	15[e]	12
PC101	TK	A	violet	558	8[e]	14
PC101A	TK	A	violet/pink	554	11	16
PC102	TK	A	violet	559	12[e]	16
(Merck)	Merck	A	l. violet	565	169[e]	38
ST41	Ishihara	A	l. violet	572	208[e]	35
(Aldrich_a)	Aldrich	A	l. violet/pink	567	217[e]	34
P25	Degussa	A/R	d. violet/pink	552	28[e]	21
(UFR)	NCU	R	d. violet/pink	546	5[e]	16
TIO6	CSJ	R	d. violet/pink	549	15[e]	19
STG1	ST	R	violet	580	250[e]	43
STF10	ST	R/A	violet	568	150[e]	25
(Aldrich_r)	Aldrich	R/A	l. grey	593	517[e]	60
TIO5	CSJ	R/A	l. grey	605	570[e]	44

[a] Names in parentheses are code names in our laboratory.

[b]CSJ: Catalysis Society of Japan, NCU: Newcastle University, ST: Showa Titanium (ST series), TK: Titan Kogyo (PC series).

[c]A: anatase, R: rutile, A/R and R/A: mixture with majority of anatase and rutile, respectively.

[d]d.: dark, l.: light,

[e]Values measured and reported previously[23]

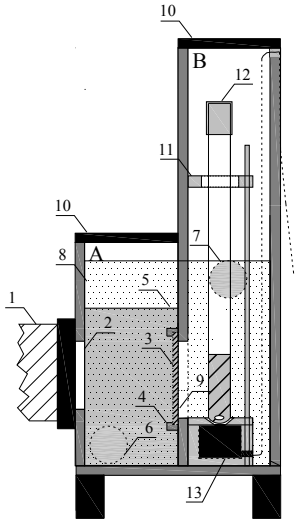

Fig. 1 Schematic drawing of experimental setup (side view) for photocatalytic activity test: 1: xenon lamp, 2: pyrex glass window, 3: cut-off filter, 4: filter holder, 5: separating wall for water circulation, 6: water inlet, 7: water outlet, 8: water bath, 9: hole for circulating water, 10: reactor covers, 11: sample tubes holder, 12: sample tubes (two), 13: stirrers (two).

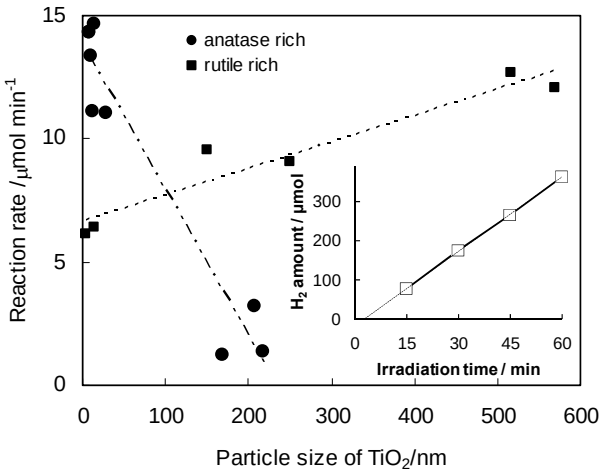

Fig. 2 Dependence of reaction rate of methanol dehydrogenation on the particle size of TiO_2. (Inset) Exemplary H_2 evolution during Au deposition on Au/TIO_2(TIO6).

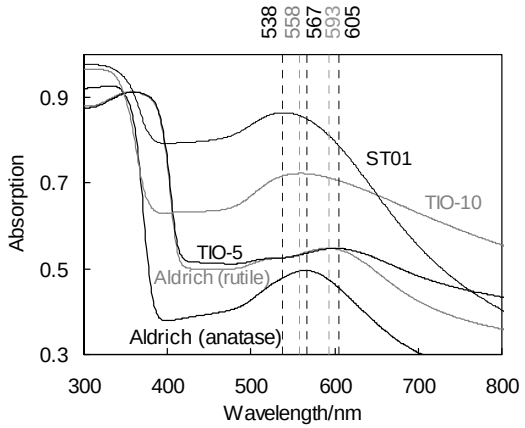

Fig. 3 Exemplary absorption spectra of Au/TiO_2s.

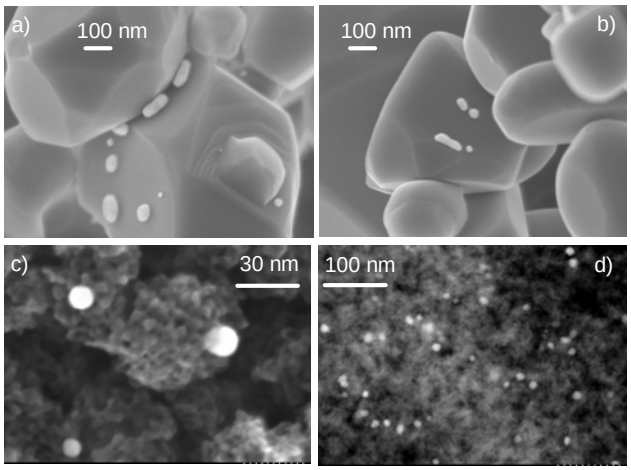

Fig. 4 SEM (a, b) and STEM (c, d) images of Au/TiO_2: a) Aldrich_r; b) TIO5; c, d) ST-01.

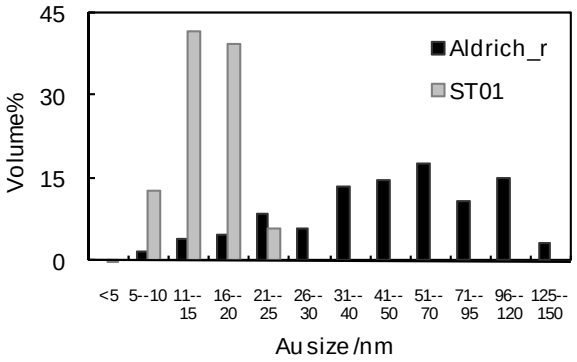

Fig. 5 Distribution of size of Au deposits on Au/TiO_2, where the volumetric content was calculated assuming constant thickness (diameter) of rod-like (spherical) Au particles.

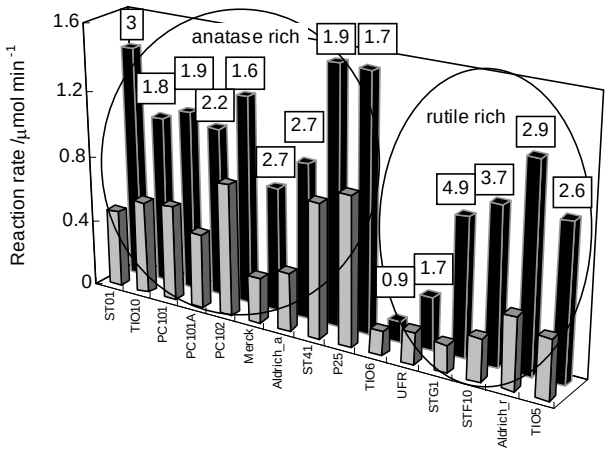

Fig. 6 Comparison of rate of photocatalytic CO_2 evolution from suspensions containing acetic acid under UV irradiation by bare (front) and gold-modified (back) titania particles. Figures in boxes show the enhancement ratio (see text)

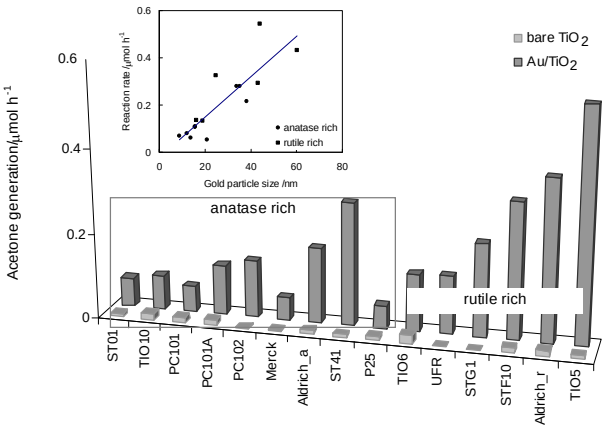

Fig. 7 Rate of photocatalytic acetone evolution from suspensions containing 2-propanol under vis irradiation (mercury lamp > 450 nm) by bare and gold-modified titania particles. (Inset)[13d] Activity dependence on gold particle size.

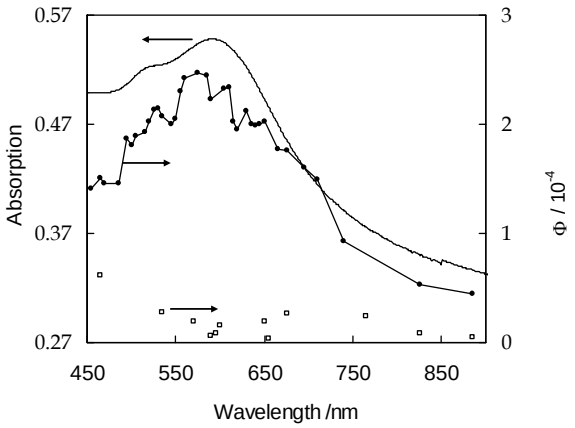

Fig. 8. Action spectrum of 2-propanol oxidation on TiO_2 (Aldrich_r): ● Au-modified, □ bare, and ▬ absorption spectrum of Au/TiO_2 (Aldrich_r) measured with barium sulfate as a reference.[13d]

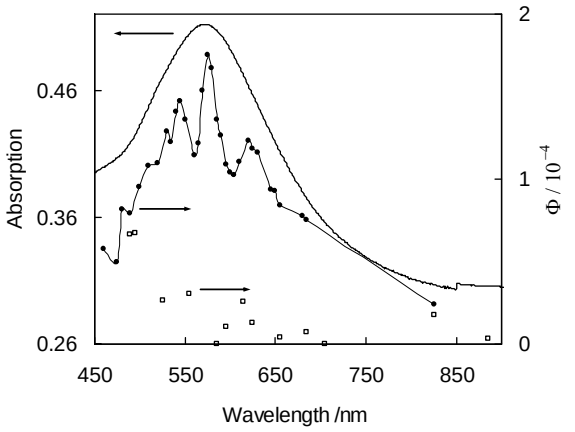

Fig. 9. Action spectrum of 2-propanol oxidation on TiO_2 (ST41): ● Au-modified, □ bare, and ▬ absorption spectrum of Au/TiO_2 (ST41) measured with barium sulfate as a reference.

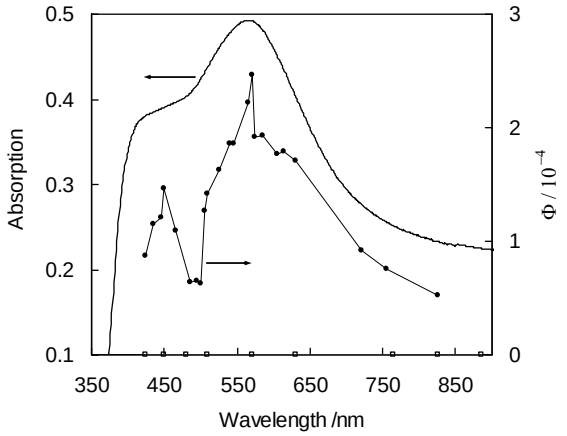

Fig. 10. Action spectrum of 2-propanol oxidation on TiO_2 (Aldrich _a): ● Au-modified, □ bare, and ▬ absorption spectrum of Au/TiO_2 (Aldrich_ a) measured with bare Aldrich_a as a reference.

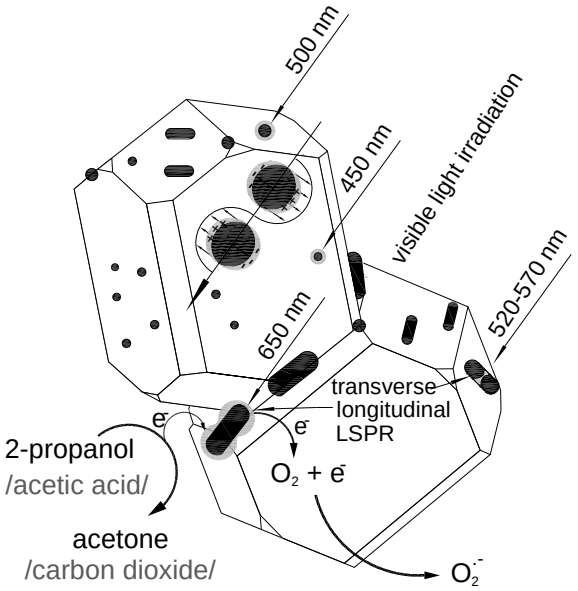

Fig. 11. Schematic representation of the mechanism of OCs oxidation by Au/TiO_2 under vis irradiation.

Notes and references

[a] *Catalysis Research Center, Hokkaido University, North 21, West 10, Sapporo 001-0021, Japan. Fax: +81–11–706–9133; Tel: + 81–11–706–9132; E-mail: kowalska@cat.hokudai.ac.jp*

[b] *Department of Chemical Technology, Gdansk University of Technology, ul. Narutowicza 11/12, Gdansk 80-952, Poland. Fax: +48–58–347–2065; Tel: +48–58–347–2637*

§ Present address: Institut für Anorganische Chemie, Universität Erlangen-Nürnberg, Egerlandstr.1. D-91058 Erlangen, Germany

† Electronic Supplementary Information (ESI) available: Preparation, characterization (STEM, absorption spectra) and activities of Au/TiO_2 and Au/SiO_2 powders prepared by impregnation/reduction method, light emission spectra of mercury and xenon lamps, the activity increase after gold deposition for acetic acid decomposition. See DOI: 10.1039/b000000x/

1 M. Lindner, J. Theurich and D. W. Bahneman, *Wat. Sci. Technol.*, 1997, **35**, 79.

2 B. Ohtani, *Chem. Lett.*, 2008, **37**, 216.

3 B. Ohtani, R. M. Bowman, D. P. Kolombo, H. Kominami, H. Noguchi and K. Uosaki, *Chem. Lett.*, 1998, **27**, 579.

4 (a) M. Bellardita, M. Addamo, A. Di Paola and L. Palmisano, *Chem. Phys.*, 2007, **339**, 94; (b) R. Gomez, T. Lopez, E. Ortiz-Islas, J. Navarrete, E. Sanchez, F. Tzompanztzi and X. Bokhimi, *J. Mol. Catal. A: Chem.*, 2003, **193**, 217; (c) R. Asahi, T. Morikawa, T. Owaki, K. Aoki and Y. Taga, *Science*, 2001, **293**, 269; (d) B. Kosowska, S. Mozia, A. W. Morawski, B. Grzmil, M. Janus and K. Kalucki, *Sol. Energy Mater. Sol. Cells*, 2005, **88**, 269.

5 (a) Y. Cho and W. Choi. *J. Photochem. Photobiol., A*, 2002, **148**, 129. (b) A. Zaleska, P. Gorska, J. W. Sobczak. and J. Hupka, *Appl. Catal. B-Environ.,* 2007, **76**, 1.

6 (a) S. Sakthivel, M. Janczarek and H. Kisch, *J. Phys. Chem., B*, 2004, **108**, 19384. (b) B. Wawrzyniak, A. W. Morawski and B. Tryba, *Int. J. Photoenergy*, 2006, 68248. (c) A. Zaleska, P. Gorska, J. Sobczak and J. Hupka, *Appl. Catal. B-Environ.,* 2007, **76**, 1.

7 (a) T. Ohno, M. Akiyoshi, T. Umebayashi, K. Asai, T. Mitsui and M. Matsumura, *Appl. Catal. A-Gen.,* 2004, **265**, 115; (b) T. Umebayashi, T. Yamaki, S. Tanaka and K. Asai, *Chem. Lett.*, 2003, **32**, 330; (c) X. Yan, T. Ohno, K. Nishijima, R. Abe and B. Ohtani, *Chem. Phys. Lett.*, 2006, **429**, 606.

8 (a) S. Sakthivel and H. Kisch, *Angew. Chem.-Int. Edit.,* 2003, **42**, 4908; (b) G. Wu, T. Nishikawa, B. Ohtani and A. Chen, *Chem. Mater.,* 2007, **19**, 4530; (c) P. Gorska, A. Zaleska, E. Kowalska, T. Klimczuk, J. W. Sobczak, E. Skwarek, W. Janusz and J. Hupka, *Appl. Catal. B-Environ.,* 2008, **84**, 440.

9 (a) W. Zhao, W. Ma, C. Chen, J. Zhao and Z. Shuai, *J. Am. Chem. Soc.,* 2004, **126**, 4782; (b) A. Zaleska, J. W. Sobczak, E. Grabowska and J. Hupka, *Appl. Catal. B-Environ.*, 2008, **78**, 92;

10 (a) P. Pichat, J. M. Herrmann, J. Disdier, H. Courbon and M. N. Mozzanega, *Nouv. J. Chim.*, 1981, **5**, 627; (b) B. Ohtani, K. Iwai., S.-i. Nishimoto and S. Sato*, J. Phys. Chem.*, 1997, **101**, 3349.

11 R. Abe, H. Takami, N. Murakami and B. Ohtani, *J. Am. Chem. Soc.*, 2008, **130**, 7780.

12 (a) W. Macyk, G. Burgeth and H. Kisch, *Photochem. Photobiol. Sci.*, 2003, **2**, 322; (b) G. Burgeth and H. Kisch, *Coord. Chem. Rev.*, 2002, **230**, 41; (c) E. Kowalska, H. Remita, C. Colbeau-Justin, J. Hupka and J. Belloni, *J. Phys. Chem., C*, 2008, **112**, 1124.

13 (a) Y. Tian and T. Tatsuma, *J. Am. Chem. Soc.*, 2005, **127**, 7632; (b) V. R. Gonzales, R. Zanella, G. del Angel and R. Gomez, *J. Mol. Catal. A-Chem.,* 2008, **281**, 93; (c) R. S. Sonowane and M. K. Dongare, *J. Mol. Catal. A-Chem.,* 2007, **243**, 68; (d) E. Kowalska, R. Abe and B. Ohtani, *Chem. Commun.*, 2009, **2**, 241.

14 A. J. Haes, C. L. Haynes, A. D. McFarland, G. C. Schatz, R. P van Duyne and S. Zou, *MRS Bull.*, 2005, **30**, 368.

15 (a) N. Halas, *MRS Bull.*, 2005, **30**, 362; (b) D. Pissuwan, S. M. Valenzuela and M. B Cortie, *Trends Biotechnol.*, 2006, **24**, 62; (c) H. Wang, D.W. Brandl, F. Le, P. Nordlander and N.J. Halas, *Nano Lett.*, 2006, **6**, 827-832.

16 D. Chatterjee and S. Dasgupta, *J. Photochem. Photobiol. C*, 2005, **2-3**, 186.

17 S. Hwang, M.C. Lee and W. Choi, *Appl. Catal. B-Environ.*, 2003, **46**, 49.

18 H.E. Chao, Y.U. Yun, H.U. Xingfang and A. Larbot, *J. Eur. Ceram. Soc.*, 2003, **23**, 1457.

19 (a) B. Ohtani, S.-W. Zhang, T. Ogita, S. Nishimoto and T. Kagiya, *J. Photochem. Photobiol. A*, 1993, **71**, 195; (b) T. Torimoto, N. Nakamura, S. Ikeda and B. Ohtani, *Phys. Chem. Chem. Phys.*, 2002, **4**, 5910.

20 Y. Zhu, Y. Qian, H. Huang, M. Zhang and S. Liu, *Mater. Lett.*, 1996, **28**, 259.

21 A. El-Azab, S. Gan and Y. Liang, *Surf. Sci.*, 2002, **506**, 93.

22 D. Andreescu, T. Kumar Sau and D. V. Goia, *J. Colloid Interf. Sci.,* 2006, **298**, 742.

23 (a) O. O. Prieto-Mahaney, N. Murakami, R. Abe and B. Ohtani, *Chem. Lett.*, 2008, **38**, 238; (b) O. O. Prieto-Mahaney, N. Murakami, R. Abe and B. Ohtani, *Phys. Chem. Chem. Phys.*, in preparation.

24 H. Irie, S. Washizuka, Y. Watanabe, T. Kako and K. Hashimoto, *J. Electrochem. Soc.*, 2005, **152,** E351.

25 (a) R. Joerger, R. Gampp, A. Heinzel, W. Graf, M. Kohl, P. Gantenbein and P. Oelhafen, *Sol. Energy Mater. Sol. Cells*, 1998, **54**, 351; (b) Y. Xia, Y. Xiong, B. Lim and S. E. Skrabalak, *Angew. Chem.-Int. Edit.*, 2009, **48**, 60; (c) J. Zhu, L. Huang, J. Zhao, Y. Wang, Y. Zhao, L. Hao and Y. Lu., *Mater. Sci. Eng. B-Solid State Mater. Adv. Technol.*, 2005, **121**, 199; (d) S. Dhara, R. Kesavamoorthy, P. Magudapathy, M. Premila, B. K. Panigrahi, K. G. M. Nair, C. T. Wu, K. H. Chen and L. C. Chen, *Chem. Phys. Lett.*, 2003, **370**, 254; (e) J.-E. Park, T. Momma, T. Osaka, *Alectrochim. Acta*, 2007, **52**, 5914.

26 K. Esumi, S. Sarashina and T. Yoshimura, *Langmuir*, 2004, **20**, 5189.

27 J. Sharma and K. P. Vijayamohanan, *J. Colloid Interf. Sci.*, 2006, **298**, 679.

28 (a) L. M. Liz-Marzan and A. P. Philipse, *J. Colloid Interf. Sci.*, 1995, **176**, 459. (b) J. Yang, J. C. Wu, K. Wang and C. C Chen, *Chem. Phys. Lett.*, 2005, **416**, 215.

29 (a) A. M. Schwartzberg., T. Y. Olson, C. E. Talley and J. Z. Zhang, *J. Phys. Chem.* B, 2006, **110**, 19935; (b) D. Andreescu, T. K. Sau and D. V. Goia, *J. Colloid Interf.* Sci., 2006, **298**, 742; (c) C. J. Orendorff, T. K. Sau and C. J. Murphy, *Small*, 2006, **5**, 636.

30 B. K. Min, W. T. Wallance, D. W. Goodman, *Surf. Sci.*, 2006, **600**, L7.

31 (a) A. Sclafani and J. M. Herrmann, *J. Phys. Chem.,* 1996, **100**, 13655; (b) O. Carp, C. L. Huisman and A. Reller, *Prog. Solid State Chem.*, 2004, **32**, 33; (c) A.G. Thomas, W.R.

Flavell, A. K. Mallick, A. R. Kumarasinghe, D. Tsoutsou, N. Khan, C. Chatwin, S. Rayner, G. C. Smith, R. L. Stockbauer, S. Warren, T. K. Johal, S. Patel, D. Holland, A. Taleb and F. Wiame, *Phys. Rev. B*, 2007, **75**, 035105.

32 A. V. Awate, A. A. Belhekar, S. V. Bhagwat and N. M. Gupta, *Int. J. Photoenergy*, 2008, DOI:10.1155/2008/789149.

33 V. Rodriguez-Gonzales, R. Zanela, G. del Angel and R. Gomez, *J. Mol. Catal. A-Chem.*, 2008, **281**, 93.

34 T. Kiyonaga, M. Fujii, T. Akita, H. Kobyashi and H. Tada, *Phys. Chem. Chem. Phys.*, 2008, **10**, 6553.

35 A. Fujishima, K. Hashimoto and T. Watanabe, *TiO_2 Photocatalysts Fundamentals and Applications*, BKC, Inc., Tokyo, 1999, ch. 8, 126.

36 L. M. Molina, M. D. Rasmussen and B. Hammer, *J. Chem. Phys.*, 2004, **120**, 7673.

37 T. Minato, T. Susaki, S. Shiraki, H. S. Kato, M. Kawai and K.-i. Aika, *Surf. Sci.*, 2004, **556-558**, 1012.

38 L. Du, A. Furube, K. Yamamoto, K. Hara, R. Katoh and T. Tachiya, *J. Phys. Chem. C*, 2009, **113**, 6454.

39 H. Wang, D. W. Brandl, F. Le, P. Nordlander and N. J. Halas, *Nano Lett.*, 2006, **6**, 827.

40 (a) M. Haruta, N. Yamada, T. Kobayashi and S. Iijima, *J. Catal.*, 1989, **115**, 115. (b) M. Valden, X. Lai and D. W. Goodman, *Science*, 1998, **281**, 1647. (c) M. S. Chen and D.W. Goldman, *Science*, 2004, **306**, 252. (d) F.-Z. Su, L. He, Y. Cao, H.-Y. He and K.-N. Fan, *Chem. Commun.*, 2008, 3531.

41 R. Joerger, R. Gampp, A. Heinzel, W. Graf, M. Kohl, P. Gantenbein and P. Oehafen, *Sol. Energy Mater. Sol. Cells*, 1998, **54**, 351.

42 V. Subramanian, E.E. Wolf and P. V. Kamat, *J. Am. Chem. Soc.*, 2004, **126**, 4943.

43 A. Orlov, D. A. Jefferson, M. Tikhov and R. M. Lambert, *Catal. Commun.*, 2007, **8**, 821.

44 E. C. H. Sykes, F. J. Williams, M. S. Tikhov and R. M. Lambert, *J. Phys. Chem. B*, 2002, **106**, 5390.

45 B. Ohtani, *Shokubai* (Journal of Catalysis Society of Japan), 2005, **47**, 301.

46 A. L. Gonzales, J. A. Reyes-Esqueda and C. Noguez, *J. Phys. Chem. C*, 2008, **112**, 7356.

47 M. Estphalen, U. Kreibig, J. Rostalski, H. Luth and D. Meissner, *Sol. Energy Mater. Sol. Cells*, 2000, **61**, 97.

48 A. Furube, L. Du, K. Hara, R. Katoh and M. Tachiya, *J. Am. Che. Soc.*, 2007, **129**, 14852.

49 N. Sakai, Y. Fujiwara, Y. Takahashi and T. Tatsuma, *Chem. Phys. Chem.*, 2009, **10**, 766.

50 D. E. Evanhoff, Jr., R. L. White and G. Chumanov, *J. Phys. Chem. B.,* 2004, **108**, 1522.

51 A. Ohnuma, R. Abe, T. Shibayama and B. Ohtani, *Chem. Commun.,* 2007, 3491.

52 C. Douketis, V. M. Shalaev, T. L. Haslett, Z. Wang and M. Moskovits, *J. Electron Spectrosc. Relat. Phenom.*, 1993, **64/65**, 167.

53 X. Chen, H.-Y. Zhu, J.-C. Zhao, Z.-F. Zheng and X.-P. Gao, *Angew. Chem.-Int. Edit.,* 2008, **47**, 5353.

54 N. Murakami, O. O. Prieto Mahaney, R. Abe, T. Torimoto and B. Ohtani, *J. Phys. Chem. C*, 2007, **111**, 11927.